Mechanical parameters identification of keloid and surrounding healthy skin using Digital Image Correlation measurements *in vivo*

A. ELOUNEG[a], D. SUTULA[a, b], M. SENSALE[a, c], F. CHOULY[d], J. CHAMBERT[a], A. LEJEUNE[a], D. BAROLI[c], P. HAUSEUX[c], S. BORDAS[c], E. JACQUET[a, ★],

a. Univ. Bourgogne Franche Comté, FEMTO-ST institute, UFC/CNRS/ENSMM/UTBM, Departement of Applied Mechanics, Besançon, France.
b. Technical University of Liberec, Faculty of Tissue Engineering, Liberec, Czech Republic.
c. University of Luxembourg, Institute of Computational Engineering, Luxembourg.
d. Univ. Bourgogne Franche Comté, Institut de Mathématiques de Bourgogne, Dijon, France.
★ Corresponding author, emmanuelle.jacquet@univ-fcomte.fr

Résumé :

La peau humaine se comporte comme une membrane élastique précontrainte. La présence de sites anatomiques favorables à l'apparition de certaines tumeurs, une chéloïde dans notre cas, alors que d'autres en sont systématiquement dépourvus atteste de l'importance de l'environnement mécanique du tissu. Par conséquent, une caractérisation de la peau avec tumeur est nécessaire pour comprendre l'expansion de la chéloïde d'un point de vue mécanique. Notre cas d'étude consiste à modéliser une structure biphasique composée d'une chéloïde entourée d'une peau saine située sur le haut du bras gauche d'une jeune femme. En combinant les données expérimentales d'un test d'extension comprenant des mesures de forces et déplacements issues de capteurs et des champs de déplacements obtenus par corrélation d'images numériques, nous réalisons une analyse mécanique pour caractériser les champs des contraintes dans tout le domaine et à l'interface 'chéloïde/peau-saine'. Sachant que le comportement mécanique d'une peau avec tumeur est inconnu, plusieurs modèles physiques peuvent être implémentées facilement dans un code numérique pour adapter les simulations aux observations. Après avoir identifié les paramètres matériau grâce à la résolution du problème inverse, les champs des contraintes sont obtenus via le post-traitement. Les prochaines étapes consistent à déterminer les directions préférentielles afin de définir aussi précisément que possible le cahier des charges d'un dispositif mécanique de prévention du développement des chéloïdes.

Abstract :

The human skin behaves as an elastic membrane initially prestressed but not uniformly. The presence of anatomical sites favorable to the appearance of some tumors, a keloid in our case, while other sites never develop them attests to the importance of the mechanical environment of the tissue. Thus, a mechanical characterization of the tumored skin is necessary to understand the keloid expansion from

a mechanical point of view. Our case study consists in modeling a bi-material structure composed of a keloid skin surrounded by healthy skin located on upper left arm of a young female. From the experimental measurements in vivo, by combining force sensor, displacement sensor and Digital Image Correlation techniques, we perform a mechanical analysis to characterize the mechanical stress fields over the entire area and on the interface 'healthy skin/keloid skin'. Since the mechanical behavior of the tumorous skin is unknown, many physical models can be implemented and assessed very easily inside the specific digital software to fit with the real data. Once a set of mechanical parameters for both the healthy skin and the keloid skin are identified, the stress fields around the keloid are calculated. Next steps consist in determining matching preferential directions in order to define as precisely as possible the specifications of a device for preventing the growth of keloids.

Keywords : keloid, parameter identification, Digital Image Correlation, Finite Element Model Updating.

1 Introduction

Our problem consist in identifying realistic parameters of a bi-material structure by using both force sensor and Digital Image Correlation measurements *in vivo*. There are many applications where this problem is important. for example, keloid growth beyond original defect margin have been linked to several supposed mechanisms which include skin mechanical properties [1],[2]. Moreover, given the fact that specific anatomic sites submitted to high forces and usual body movements are known to be pro-keloid sites [3], researchers have been encouraged to focus on mechanical behaviour of such structures. The main target of the paper is to develop the generic methodology used to identify the mechanical properties of the tumored skin. The whole procedure from *in vivo* experimental test to stress field computation would be described. The corresponding displacement field is measured by Digital Image Correlation on both healthy skin and keloid skin separetely, and the reaction forces by sensors. Then, an inverse method, known as Finite Element Model Updating (FEMU) based on the inverse least square method, is performed on these data. The completed model with successfully identified parameter will be used finally to calculate the stress field. Hereafter, the experimental device and the uniaxial measurements are described. Then, a numerical modeling is presented and resulting parameters are provided. The originality of the method consists in an objective function built from displacement fields and taking into account the reaction force value necessary to extension test as a constraint. In conclusion, several improvements are explained.

2 Materials

2.1 Uniaxial tensile test

The keloid specimen investigated is a butterlfly-shaped keloid scar located on the upper left arm of a young Caucasian female (figure 1a). Healthy skin reference on the contralateral site is investigated as an homogeneous reference material. Mean values of the thickness of each structure composed of healthy skin or keloid skin have been obtained by high frequency ultrasound. An uniaxial extension test has been conducted with an ultra-light homemade portable extensometer which minimizes the disturbance of measuring area induced by peripheral zones. Two double pads are sticked on the *in vivo* skin surface.

(a) Magnified Butterfly-shaped keloid
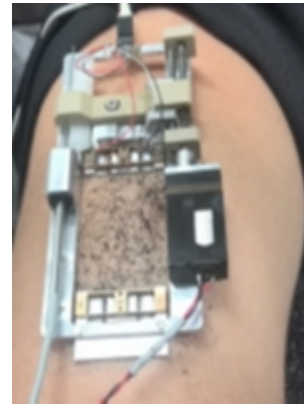
(b) DIC Speckle pattern onto healthy skin

Figure 1: Uniaxial tensile testing on keloid-skin

The extension consists in moving one pad in opposite direction to the other one, which remains static, with a controlled servomotor. The reaction force on the moving pad is measured by a strain gauge sensor. A high resolution camera is synchronized to the mechanical test to record the loaded area during the test. For image correlation clarity reasons, a speckle pattern is applied onto the skin within an area of interest (figure 1b).
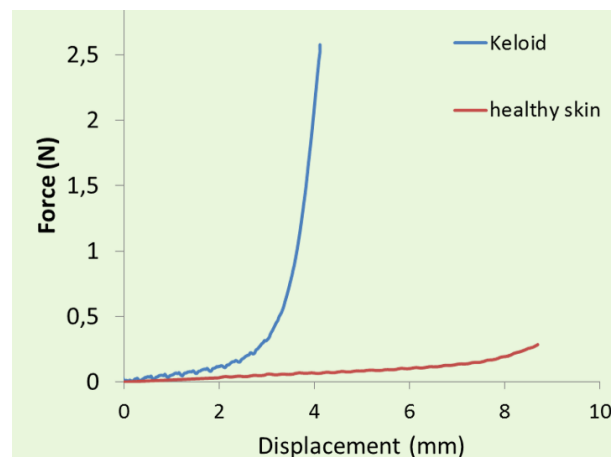

Figure 2: Force-Displacement curve during extension test

2.2   Experimental data

The mean value of healthy skin thickness is $1.46 +/- 0.1mm$ measured by analyzing ultrasound images. Whereas, the mean value of keloid skin thickness is $2.93 +/- 1.26mm$. The extension test provides the reactional force values exerted on the measurement pads and the displacement between the pads during all the mechanical tests (Figure 2). The displacement fields of the zone of interest have been identified by digital image correlation. X-displacement field and Y-displacement field for healthy skin are shown on figure (3). Note that the zone of interest covers all the area located between the two double-pads 3× larger than the one submitted to a quasi-traction test [4]. Hence, these two kinds of measurement data, reactional force and displacement fields, are the exprimental inputs of our numerical model that will be used to identify the physical model.
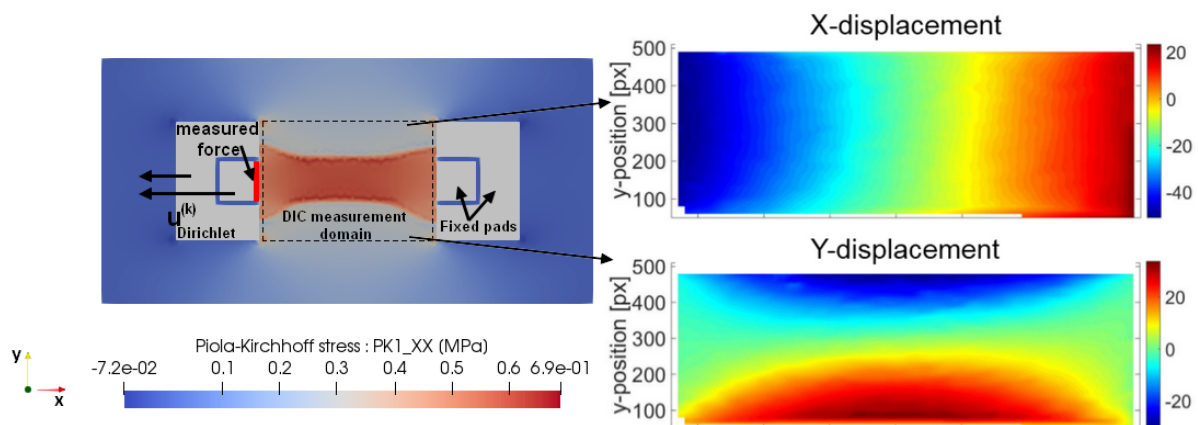
Figure 3: Experimental data of keloid-skin undergoing large deformation

3   Methods

3.1   Process scheme

We recall that the main objective of this work is producing somehow a 'black box' which identify the physical parameters of the keloid, by taking in account obviously the behavior of the peripheral healthy skin. As shown in figure (4), the numerical tool adapted of the uniaxial tensile test can deal with many multi-material models since the geometry and the behavior law are part of the inputs, which makes it more flexible so far. The whole procedure of the inverse identification problem would be described. As the corresponding displacement field is measured by Digital Image Correlation and the reactional force by sensors, experimental data need to be filtered to reduce measurement noise. Then, an inverse method, known as Finite Element Model Updating (FEMU) containing, is performed on these data. In addition, the objective cost function (ref the equation) takes account of the difference between numerical and experimental reaction force as a constraint. The most interesting sub-blocks of the FEMU algorithm are the non-linear FEM solver and the inverse solver. By setting an initial guess of the parameters, the displacements over the nodes are computed for each load step $k = 1, 2, ..., N_E$ by solving the variational problem below

$$F(u^{(k)}; v) = 0 \quad \forall v \in V \tag{1}$$

where V is a suitable function space of admissible virtual displacement that satisfies boundary conditions on $\boldsymbol{u}$, and F is the variational form of the quasi-static equilibrium

$$F(u; v) = \frac{d\Pi(u + \epsilon v)}{d\epsilon}\bigg|_{\epsilon=0} \tag{2}$$

Π is total potential energy, it's given by

$$\Pi = \int_\Omega \psi(u)dx - \int_\Omega B \cdot dx - \int_{\partial\Omega} T \cdot ds \tag{3}$$

B and T are respectively the body and the traction forces. In our uniaxial tensile test configuration, they are null. While ψ is the elastic strain energy density which characterizes the behavior law of the materials. We need to set it as an input data, because the main issue of fitting with the experimental force-stretch curve is the choice of the behavior equation. On the other hand, by linking the simulated displacement fields to the experimental ones through the optimization formulation, the inverse solver
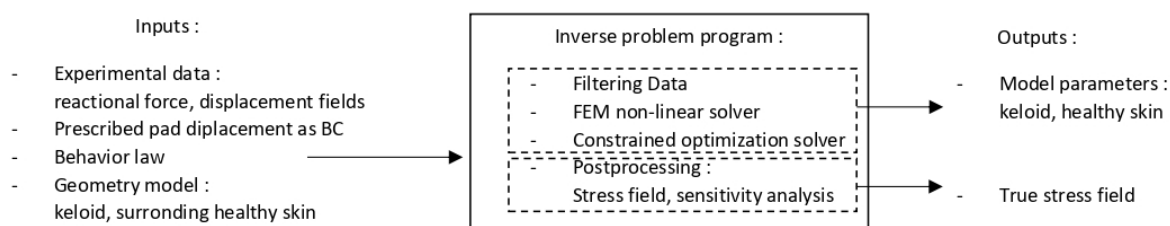
Figure 4: Process scheme of the inverse problem

allows us to find the best set of material parameters that minimize the objective function as detailed in section 3.3. The introduced software program above was written in Python using the packages of *FEniCS Project*. The latter is a collection of free and open-source software components, it's used commonly to solve finite-element variational formulation of ODEs and PDEs.

3.2 Constitutive model

Many recent studies showed that the biological soft tissues, human skin for instance, behave as a hyperelastic material. According to Limbert's review ([5]), the mathematical and computational models of the human skin can be classified into three main categories : phenomenological, structural and structurally based phenomenological models. The first one is purely mathematical, the microstructure and multiple phases as well their associated mechanical properties are ignored. If one considers mechanical behaviour only, a phenomenological model is a set of mathematical relations that describe the evolution of stress as a function of strain, not linearly most of time. It is generally always possible to fit such a constitutive law to a set of experimental data. This approach has two major drawbacks : the resulting constitutive parameters often do not have a direct physical interpretation, and the displacement solution obtained by minimizing the strain energy can be not unique. Although, our objective is to determine the stress field whatever the nature of the behavior law that fit to the experimental curve. We choose to implement then a phenomenological model in our program [6]. The other classes of constitutive models can be theoretically input into the numerical model, but they contains too many parameters, which may increase horrifically the computation cost. The underlying assumptions for both materials, healthy skin and keloid, should be the same. In other words, they present the same behavior law but different parameters. We assume that theses soft tissues are hyperelastic, homogenoeus and isotropic. Their large deformations are assumed to be quasi-static.

3.3 Inverse identification

The objective function used to identify the material parameters $\theta = \{\theta_{healthy\,skin}; \theta_{keloid}\}$ is the sum over all loading time steps of the absolute difference between the predicted and the experimental displacements, by taking account of the difference between the predicted forces, calculated from the simulated displacements, and the ones gathered from the test. An additional parameter Lagrange multiplier links the two mismatches. The $N_\theta + 1$ parameters are calculated by minimizing the following term

$$J(\theta, \lambda) = \sum_{k=1}^{N_E} \int_{\Gamma_{\text{msr}}^u} \left(u^{(k)}(\theta) - u_{\text{msr}}^{(k)} \right)^2 dx + \lambda \int_{\Gamma_{\text{msr}}^f} \left(f(u^{(k)}(\theta), \theta) - f_{\text{msr}}^{(k)} \right) dx \qquad (4)$$

with Γ_{msr}^{u} a part of the domain Γ_E where the displacement field is measured (i.e. using DIC) and Γ_{msr}^{f} the boundary where the force is measured using deformation gauge. Among many non-linear least squares methods detailed in Harb's Thesis [7], we have selected Newton-Gauss algorithm to be implemented into the inverse solver. The latter method is enough accurate and not so expensive providing that we set a valid initial guess of the material parameters.

3.4 Validation

The entire inverse problem numerical tool is validated in two steps. First of all, we validate separately the FEM non-linear solver by comparing the nodal solutions vis-à-vis commercial FEM codes, *COMSOL MULTIPYSICS* and *ANSYS*, and the inverse solver by using the simulated data as the experimental inputs (The material parameters values used for making data are computed through the inverse solver factory). By fixing randomly values too much far from the targeted parameters (up to ×500), the inverse solver was able to converge to the right set of parameters with reasonable number of iterations. Secondly, the computations are performed on real data. We have chosen the alternative compressible hyperelastic Neo-Hookean model (5) as an input behavior law to make it simpler for validation. Moreover, the deformed structure shape deriving from the response of the Neo-Hookean model is so realistic as shown in figure (5). Consequently, we have identified 4 material parameters in addition to Lagrange multiplier $\theta = \{\mu_{healthy\,skin}, \lambda_{healthy\,skin}, \mu_{keloid}, \lambda_{keloid}\}$. Further behavior laws should be tested very easily such that the model is in good agreement with available observations.

$$\psi = \frac{\mu}{2}\left(I_1 - 3 - 2\ln J\right) + \frac{\lambda}{2}\left(\ln J\right)^2 \tag{5}$$
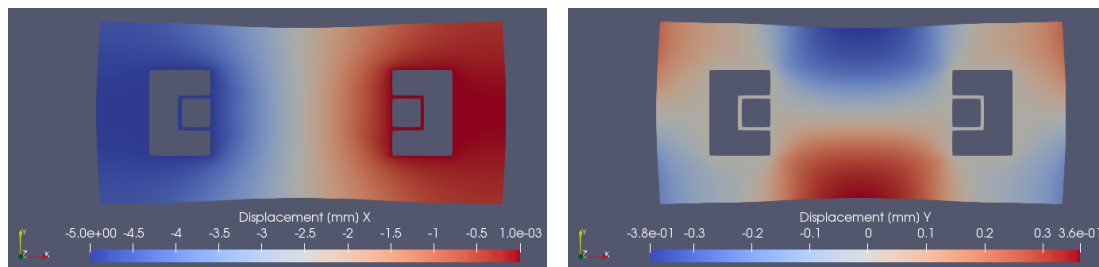

Figure 5: Predicted displacement fields of the Neo-Hookean alternative model

3.5 Postprocessing

At the end of the identification process, the parameters are again introduced into the FEM solver to simulate the model responses as close as possible to the real data. Two final operations take place then: quantifying the model parameters sensitivities with respect to the measurement noise and calculating the stress fields. The output stresses, in the form of Cauchy or Piola-Kirchhoff I (3), will help us to understand better at the first level the behavior in the interface medium healthy-skin/keloid.

4 Conclusions

Our methodology, concertized in a sophisticated open-source computational framework, is able to provide the mechanical properties, true stress field for instance, of a keloid scar. The latter is growing at the expense of the surrounding healthy skin. Thus, we developed a bi-materials model inside the program to observe the behavior on the interface zone between the keloid and the healthy skin using

the FEM Updating algorithms. The inputs to the program are the experimental data, gathered from a uniaxial test and DIC measurement, and the constitutive model as a strain energy density. We have validated and analyzed the reliability of the outputs using faked and real data. In perspectives, several phenomenological material model will be tested to provide results fitting very well with the experimental inputs. And in the long term, our valid results will help to define specifications of a device for preventing the growth of keloids.

References

[1] K.M. Ramakrishnan, K.P. Thomas, C.R. Sundararajan, Study of 1,000 patients with keloids in South India, Plast Reconstr Surg, 53 (1974) 276–280.

[2] Z. Wang, K.D. Fong, T.-T. Phan, I.J. Lim, M.T. Longaker, G.P. Yang, Increased transcriptional response to mechanical strain in keloid fibroblasts due to increased focal adhesion complex formation, J Cell Physiol, 206 (1973) 510–517.

[3] R. Ogawa, Keloid and hypertrophic scarring may result from a mechanoreceptor or mechanosensitive nociceptor disorder, Med Hypotheses, 71 (2008) 493–500.

[4] E. Jacquet, S. Joly, J. Chambert, K. Rekik, P. Sandoz, Ultra-light extensometer for the assessment of the mechanical properties of the human skin in vivo, Skin Res Technol, 23 (2017) 531–538.

[5] G. Limbert, Mathematical and computational modelling of skin biophysics: a review, Proceedings of the Royal Society A: Mathematical, Physical and Engineering Sciences 473(2017).

[6] G.A. Holzapfel, Nonlinear Solid Mechanics: A Continuum Approach for Engineering, book, 2002.

[7] N. Harb, Identification inverse de paramètres biomécaniques en hyperélasticité anisotrope, Thesis, Université de Technologie de Belfort-Montbeliard, 2013.